

Synthesis and characterization of polycaprolactone-based segmented polyurethanes

Aysun GÜNEY^{1,2}, Aysel KIZILTAY^{3,4}, Nesrin HASIRCI^{1,2,4},
Tuğba ENDOĞAN TANIR^{3,4*}

¹Graduate Department of Polymer Science and Technology, Middle East Technical University, Ankara, Turkey

²Department of Chemistry, Middle East Technical University, Ankara, Turkey

³Central Laboratory, Middle East Technical University, Ankara, Turkey

⁴BIOMATEN – METU Center of Excellence in Biomaterials and Tissue Engineering, Ankara, Turkey

Received: 15.01.2018

Accepted/Published Online: 10.12.2018

Final Version: 03.04.2019

Abstract: Segmented polyurethanes were synthesized by the reactions of poly(ϵ -caprolactone) (PCL)-diol and 1,6-hexamethylene diisocyanate through bulk polymerization without using solvent, initiator, or catalyst. Phase separation and hydrogen bond formation between hard segments or between hard and soft segments were examined by Fourier transform infrared spectroscopy (FTIR)-ATR and X-ray diffraction (XRD), while physical and mechanical properties were studied by atomic force microscope, differential scanning calorimeter, dynamic mechanical analysis, and tensile tester. When the diisocyanate content was increased, deconvolution results of FTIR-ATR in C=O and N-H regions demonstrated better miscibility of the segments and XRD results showed a significant decrease in the crystallinity of soft segments. Samples having strong hard segment interactions displayed better mechanical properties.

Key words: Segmented polyurethanes, poly(ϵ -caprolactone)-diol, hard segment, phase segregation, deconvolution

1. Introduction

Polyurethanes (PUs) are generally produced by the reaction of diisocyanates with polyols or diamines. Flexible macrochains of polyols have low glass transition temperature (T_g) values and form the soft segments (SS), while hydrogen bonded urethane groups form the hard segments (HS) of the polymeric network structure. These segments may be soluble in each other having a good mixing, or stay separately as domains forming segmented polyurethanes (SPUs).¹ The amounts and distributions of HS and SS affect the properties of the resultant polymer. HS provides high modulus while SS provides extensibility to the product. Hydrogen bonds between hard-and-hard segments (HS-HS) and hard-and-soft segments (HS-SS) are formed due to the presence of polar functional groups on the PU chains such as N-H and C=O groups.² The degree of miscibility of HS and SS depends on the level of H-bonding between these segments. In the cases where stronger hydrogen bonding occurs between HS and HS, phase separation becomes dominant which leads to high performance materials.^{3,4} Phase mixing occurs by strong intra- or intermolecular interactions between HS and SS, which significantly reduces mechanical properties of the end product. SPUs having different properties can be obtained by varying the type and the amounts of initial components, by using different molecular weight diol component, or by changing the preparation process. All these change the amounts and distribution of the HS and SS and lead to variation

*Correspondence: endogan@metu.edu.tr

in the final properties. Versatility of physical and mechanical properties makes these polymers attractive in industrial applications⁵ as well as in medical applications. There are various PUs studied as cardiovascular implants,⁶ tissue scaffolds,⁷ drug delivery devices,⁸ bone grafts,⁹ injectable,¹⁰ and antibacterial materials.¹¹ The ones based on poly(ϵ -caprolactone) (PCL) have been investigated as biodegradable tissue engineering scaffolds since their ester bonds are susceptible to in vivo chemical and enzymatic hydrolysis.^{12–15} In general, additives such as small molecular weight molecules of solvents or catalysts used in the synthesis may cause toxic effects by leaching out from the network structure in the biological environment.¹⁶ Therefore, in some studies, SPUs were prepared in the absence of these ingredients.¹⁷ It is also reported that SPUs prepared without using any catalyst demonstrated much less amount of side reactions and higher biocompatibility.¹⁸ Heijkants et al. synthesized SPUs by using PCL and 1,4-butane diisocyanate (BDI) in the absence of solvent and catalyst to be used as degradable meniscus scaffold.¹⁹ Polydiols having different molecular weights were used in the synthesis of PUs and it was observed that decrease in molecular weight of polyol led an increase in HS content and enhanced young modulus and mechanical properties of the final products. Bil et al. synthesized SPUs containing 22–70 wt.% HS by using different molecular weight PCL-diol, cycloaliphatic diisocyanate 4,4'-methylenebis(cyclohexyl isocyanate), and ethylene glycol as chain extender for bone tissue engineering purpose, and it was reported that when HS content increased, the surface of PU exhibited higher hydrophilicity as well as higher urethane moieties and phase separation.²⁰

In this study, various SPUs were synthesized by using aliphatic 1,6-hexamethylene diisocyanate (HDI) and PCL-diol without adding any other ingredients such as solvent, chain extender, catalyst, or initiator, so that the polymer would have different amounts of HSs (17–40 wt.%). The effects of composition on the properties of the resultant SPU were examined. The hydrogen bond-driven organizations of HS and SS domains in the polymer, as well as crystallinity and mechanical properties of the SPU samples obtained, were examined by Fourier transform infrared spectroscopy (FTIR)-ATR, atomic force microscope (AFM), differential scanning calorimeter (DSC), dynamic mechanical analysis (DMA), X-ray diffraction (XRD), and mechanical tester. Although there are some studies reporting phase segregation and properties of SPUs, in this study an aliphatic diisocyanate component was used and no ingredients were added into the reaction medium, which is especially important for medical purity. It was shown that presence and distribution of HS and SS, as well as their interactions significantly affected the macroscopic and microscopic properties of the resultant SPUs. The data obtained can be a source for the scientists and the SPUs prepared in medical purity can find applications in biomedical area.

2. Results and discussion

SPUs synthesized in this study were characterized in detail by using spectroscopic, thermal, and mechanical test techniques. Results obtained from these analyses are given below.

2.1. Results of FTIR-ATR analysis

The main characteristic peaks of SPUs are observed in the regions of 3500–3200 cm^{-1} and 1800–1600 cm^{-1} , corresponding to N–H and C=O stretching vibrations, respectively (Figure 1). Extent of hydrogen bond formation between the segments can be evaluated from FTIR-ATR spectra, and degree of microphase separation can be estimated. As the strength of hydrogen bonding increases, shifts in frequencies of N–H stretching and C=O stretching to lower frequencies occur.²¹ The arrangements of hydrogen bonds among the HS-HS indicate better phase separation while bonds among HS-SS indicate phase mixing. In order to understand

phase properties, stretching bands of N–H and C=O were deconvoluted using Peakfit Version 4.12 software. During this process, peaks were considered a Gaussian–Lorentzian sum function with a number of iterations. As a result of deconvolution, position, and area of each deconvoluted peak belonging to N–H and C=O stretching regions were calculated and the obtained data are explained below.

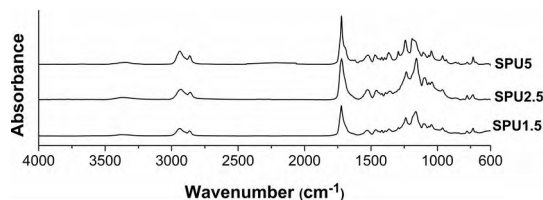


Figure 1. The FTIR spectra of the SPUs.

2.1.1. N–H stretching region

The FTIR spectra of all SPUs are given in Figure 1. The IR spectra of N–H stretching region were examined in order to identify the type of hydrogen bonding (Figure 2A). The deconvolution results for peak positions and areas of either free N–H groups or hydrogen bonded N–H groups are listed in Table 1.

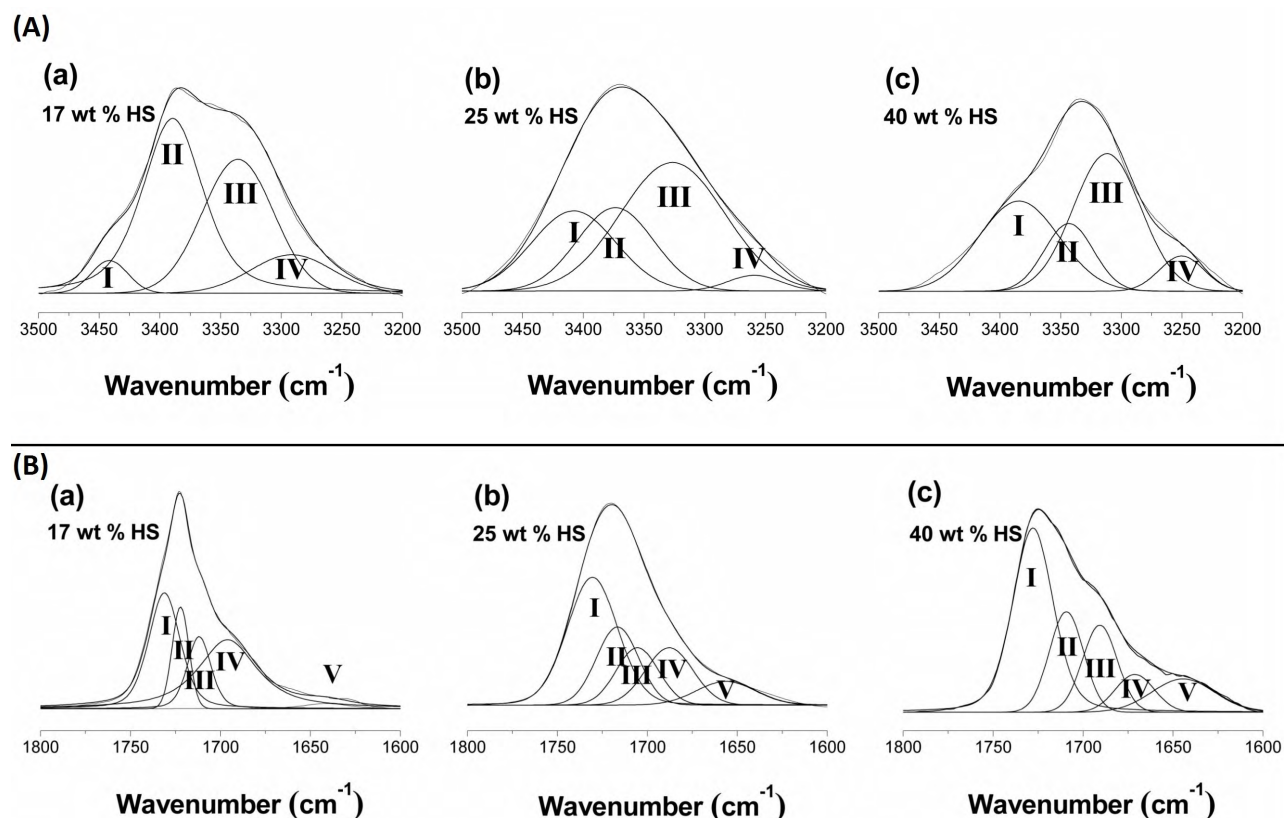


Figure 2. The deconvoluted N–H region (A) and C=O region (B) of IR spectra for all SPUs: (a) SPU1.5, (b) SPU2.5, and (c) SPU5.

Table 1. Deconvolution results of the N–H region with peak positions and percent peak areas.

	I	II	III	IV
Sample	Free	HS-HS	HS-SS	Fermi resonance
SPU1.5	3442 cm ⁻¹ 4.6%	3389 cm ⁻¹ 46.5%	3336 cm ⁻¹ 36.9%	3291 cm ⁻¹ 12.1%
SPU2.5	3409 cm ⁻¹ 24.7%	3376 cm ⁻¹ 23.4%	3331 cm ⁻¹ 48.7%	3270 cm ⁻¹ 3.2%
SPU5	3384 cm ⁻¹ 33.6%	3343 cm ⁻¹ 15.7%	3311 cm ⁻¹ 43.2%	3250 cm ⁻¹ 7.5%

Peaks I, II, and III corresponding to the free N–H, H-bonded N–H stretching between HS-HS, and H-bonded N–H stretching between HS-SS, respectively, shifted to lower frequencies as the amount of HS increased in the composition. Shifting in peak positions indicates stronger interactions due to covalent allophanate bonds and crosslinks between urethane groups, as well as a reduction in average length of hydrogen bonds. Therefore, it can be concluded that with increasing HDI amount in the polymerization reaction, strength of hydrogen bonds increases and SPU5 samples indicate the strongest H-bonds of N–H groups, since H-bonded N–H groups in HS-HS (peak II), as well as in HS-SS (peak III), appear at the lowest frequency. For peak IV, there are many definitions such as a two-phonon band,²² an overtone of deformation vibration of N–H group increased by Fermi resonance,²³ and the N–H groups bonded with the carbonyl of urethane by forming a dual-cis bond.²⁴ Representative information about phase separation cannot be attained from deconvolution of N-H peak region.

Meanwhile, a significant increase in the band areas of free N–H stretching (peak I) and decrease in the band area of the H-bonded N–H in HS-HS (peak II) was observed parallel to the increase in HS content. It can be concluded that most of the N–H groups do not take part in hydrogen bond formation while amine groups are consumed by forming allophanate linkages. When peak II and peak III are compared, SPU1.5 had higher interaction in HS-HS (46.5%) than in HS-SS (36.9%); therefore, it showed higher phase separation. On the other hand, in SPU2.5 and SPU5 samples the peak area of HS-SS was higher than that of HS-HS indicating better phase mixing compared to SPU1.5. As a result of this comprehensive analysis by deconvolution of N–H region, the order of phase separation can be given as: SPU1.5 >SPU2.5 >SPU5.

2.1.2. C=O stretching region

The carbonyl bond is elongated with the presence of hydrogen bonding and compared to the free carbonyl band, hydrogen bonded carbonyl band is observed at a lower frequency in IR spectrum.²⁵ Due to the fact that PU samples have different concentration of HS, a number of bands having different peak positions and areas were observed in the deconvoluted spectra of SPUs (Figure 2B and Table 2). The shifts in the absorbance of hydrogen bonded carbonyls in HS-HS and HS-SS to lower frequencies, similar to N-H region, demonstrate stronger hydrogen bonds among the groups. For SPU5 samples, the band area of peak I related to free carbonyl ester groups was highest (45.0%) and the band area of peak IV in the HS-HS peak related to hydrogen bonded urethane carbonyl was lowest (8.1%) compared to SPU1.5 and SPU2.5. The results support the H-bonding data obtained from the deconvolution of N–H region. Meanwhile, the band area of peak IV for SPU1.5 corresponding to hydrogen bonded groups in HS-HS was the highest (38.5%) among all SPU samples defining effective phase separation. The increase in HDI content increased the free carbonyls in ester groups of SSs, and carbonyl groups in allophanate linkages caused a decrease in the amount of H-bonded carbonyls in urethane linkages. The phase segregation order was obtained as: SPU1.5 >SPU2.5 >SPU5 similar to the order obtained from the

deconvolution analysis of N–H region. This is supported by the study of Faria et al.²⁶ They prepared various poly(urethane urea)s by varying the content of PCL-diol, and reported that HS aggregation increased parallel to the increase in PCL content.

Table 2. Deconvolution results of the C=O region with peak positions and peak areas.

	I	II	III	IV	V
Sample	(Free) Ester	(HS-SS) Ester	Free urethane	(HS-HS) Urethane	Allophanate and/or Biuret
SPU1.5	1731 cm ⁻¹ 31.6%	1722 cm ⁻¹ 13.2%	1712 cm ⁻¹ 14.7%	1696 cm ⁻¹ 38.5%	1641 cm ⁻¹ 2.0%
SPU2.5	1730 cm ⁻¹ 40.4%	1717 cm ⁻¹ 20.0%	1706 cm ⁻¹ 14.6%	1688 cm ⁻¹ 16.6%	1656 cm ⁻¹ 8.4%
SPU5	1728 cm ⁻¹ 45.0%	1709 cm ⁻¹ 18.9%	1691 cm ⁻¹ 16.6%	1671 cm ⁻¹ 8.1%	1643 cm ⁻¹ 11.4%

2.2. Results of AFM analysis

Distinct morphological features in SPUs were verified by AFM images (Figure 3). The dark areas correspond to SS-rich domains, whereas the bright ones correspond to the HS-rich domains in the PU structures. SPU1.5 possessed microphase-separated morphology with parallel oriented thread/ribbon-like structures as hard domains which dispersed in SS (Figures 3a and 3b). In the polymers with higher HS content, hard domains form more interconnected inhomogeneous and rather randomly oriented features (Figures 3c and 3d). SPU5 had highly irregular HS domains compared to SPU1.5, meaning that phase mixing is more likely than phase separation (Figures 3e and 3f). The height fluctuation ranged from -50 nm to 15 nm, from -50 nm to 40 nm, and -8nm to 12 nm for SPU1.5, SPU2.5, and SPU5, respectively. SPU5 demonstrated a subtler surface compared to SPU1.5 and SPU2.5. The surface texture significantly changed from the one with little HS domain content existing at low HS levels (17%) to that in which the polymer has an interlocking domain morphology at higher HS content (25% and 40%).

2.3. Results of DSC analysis

Thermal behavior of PCL-diol and synthesized PUs was examined by DSC (Figures 4a–4d). Mainly, T_g and melting temperature (T_m) of SS regions were characterized from DSC curves. The relative purity of these SS regions may be identified with T_g values. In the literature, it was defined that as the orientation of SS domains is disturbed with HS, the T_g value of SS shifts to higher temperatures.²⁷ It was also indicated that increase in HS content leads to an increase in the T_g value of the polymer due to the restrictions of the SS motions by HSs. Wang et al. synthesized a series of poly(ester-urethane)s with varying HS contents in the range of 25% to 41%, and reported that T_g value shifted from -31 °C to -3.2 °C.²⁸ For pure PCL-diol, T_g is about -69.4 °C. A shift to higher temperatures (up to -52.7 °C) upon formation of the SPUs was obtained in this study. However, T_g values of SSs were not significantly different from each other for the resultant SPUs. Meanwhile, T_m values significantly decreased from 52.9 °C to 21.4 °C with the increase in HDI content, indicating the devastation of the crystalline structure of PCL-diol molecules.

2.4. Results of DMA analysis

In DMA experiments, the temperature range was started from -100 °C and increased up to a value where the samples become very soft to handle. The storage modulus (E') and loss modulus (E'') values are shown

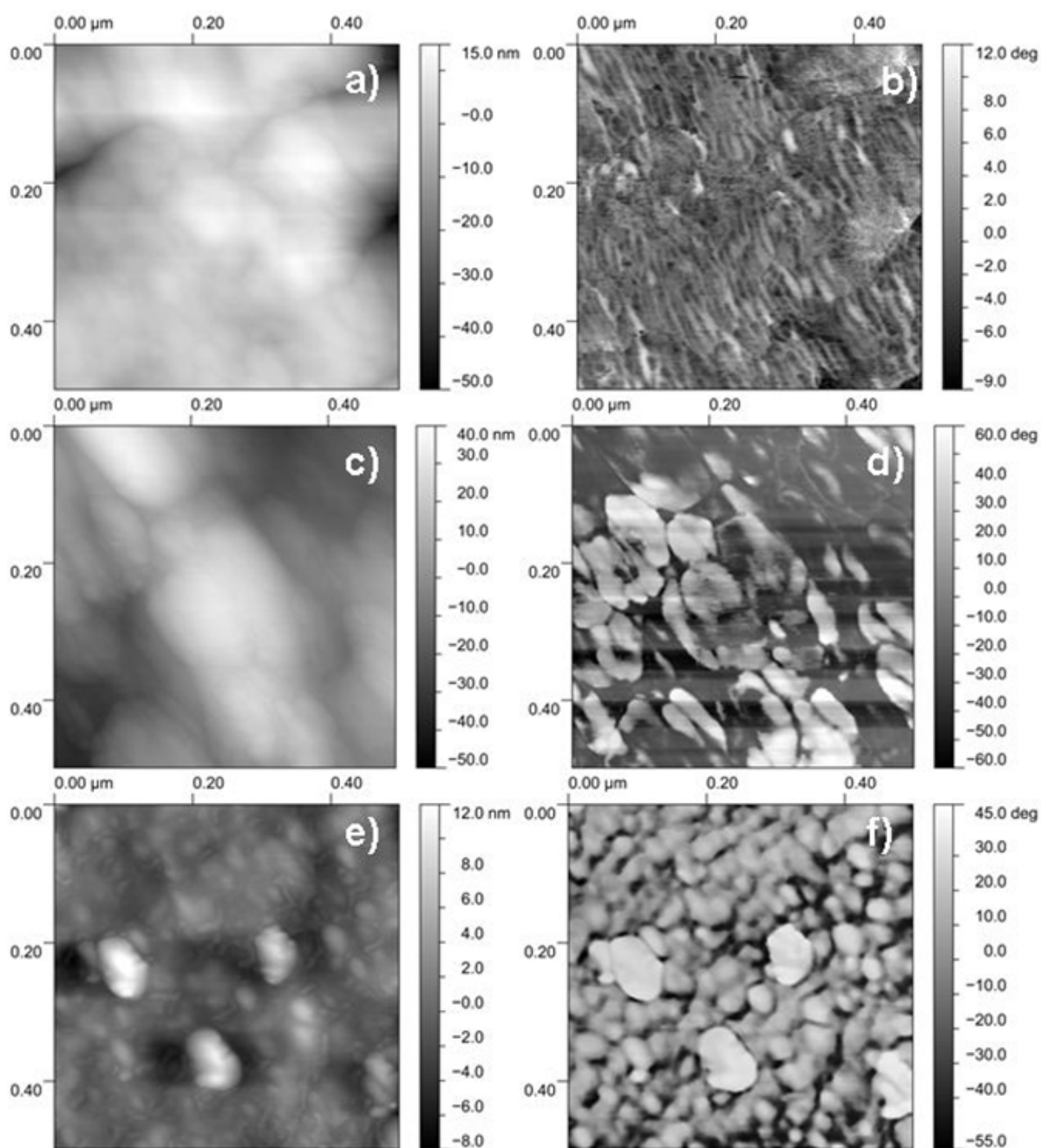


Figure 3. AFM height (left) and phase (right) images: (a, b) SPU1.5, (c, d) SPU2.5, and (e, f) SPU5.

in Figure 5, and the transition temperatures, as well as the values of E' and E'' at 25 °C and 37 °C, are tabulated in Table 3. Similar to the results obtained from IR and AFM analysis, microphase-separated nature of SPU1.5 sample was demonstrated with three mechanical relaxation processes (peaks in E') observed in DMA curves. The relaxations detected at about -53 °C, 24 °C, and 62 °C correspond to T_g of soft segment, hard-soft segment, and hard segment interactions, respectively. In addition to these relaxations, sample flow was observed at about 93 °C. Observation of three segmental relaxations indicated the existence of heterophase

morphology in SPU1.5. Two segmental relaxations were detected in DMA curve of SPU2.5 at about $-51\text{ }^{\circ}\text{C}$ and $20\text{ }^{\circ}\text{C}$ corresponding to T_g value of SS and mixed segments, respectively. Mixed segments present in SPU1.5 and SPU2.5 demonstrated partial crystallinity up to $40\text{ }^{\circ}\text{C}$. Then, sample flow took place at about $62\text{ }^{\circ}\text{C}$. In contrast to SPU1.5 and SPU2.5, highly crosslinked SPU5 sample had one relaxation at $-50\text{ }^{\circ}\text{C}$ assigned to T_g of SSs. Meanwhile, T_g of SSs remained unchanged with variation of crosslinking in SPUs. The reason is that permanent interlocking of the polymer chains restricts SS mobility. Then, in the temperature range of $11\text{ }^{\circ}\text{C}$ to $94\text{ }^{\circ}\text{C}$, a rubber plateau was observed for SPU5 sample. Different from DMA results of SPU1.5 and SPU2.5, between glassy and rubbery plateau regions SPU5 sample had a slower decaying transition region in storage modulus (E') curve due to existence of completely mixed HS-SS phases with homogeneous structure in the polymer matrix. As a consequence of multiple relaxation temperatures of SPU1.5 and SPU2.5 samples, they most likely exhibit phase-separated behavior in their structures compared to SPU5.

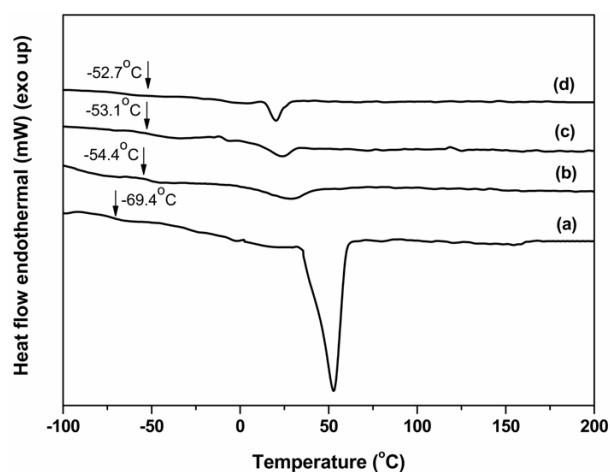


Figure 4. DSC thermograms: (a) PCL-diol, (b) SPU1.5, (c) SPU2.5, (d) SPU5.

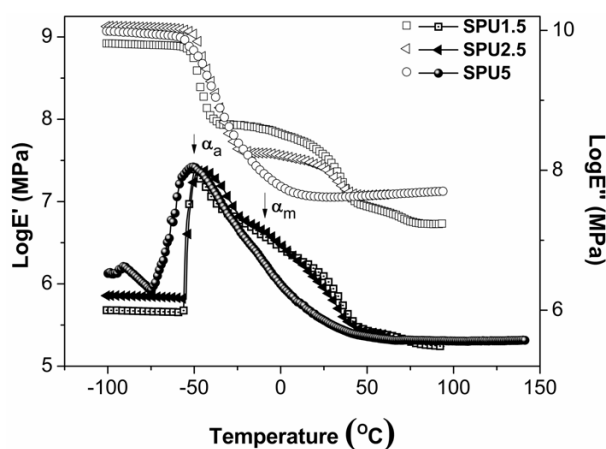


Figure 5. Temperature dependence of E' and E'' for SPUs (Conditions: $5\text{ }^{\circ}\text{C}/\text{min}$, 1 Hz , tensile mode).

Table 3. Transitions obtained from E' and E'' values at $25\text{ }^{\circ}\text{C}$ and $37\text{ }^{\circ}\text{C}$. T_{g1} : T_g of soft segment, T_{g2} : T_g of hard segment, T_{gM} : T_g of mixed phase.

Sample	Transitions (E'')			$E' \times 10^6$ at	$E' \times 10^6$ at	$E'' \times 10^6$ at	$E'' \times 10^6$ at
	T_{g1} ($^{\circ}\text{C}$)	T_{g2} ($^{\circ}\text{C}$)	T_{gM} ($^{\circ}\text{C}$)	$25\text{ }^{\circ}\text{C}$ (Pa)	$37\text{ }^{\circ}\text{C}$ (Pa)	$25\text{ }^{\circ}\text{C}$ (Pa)	$37\text{ }^{\circ}\text{C}$ (Pa)
SPU1.5	-53	62	24	37.1	15.3	3.1	1.1
SPU2.5	-51	-	20	25.2	14.5	2.1	0.7
SPU5	-50	-	-	11.3	11.5	0.7	0.5

T_{g1} : T_g of soft segment, T_{g2} : T_g of hard segment, T_{gM} : T_g of mixed phase.

It was deduced from DMA results that in the glassy region at $-100\text{ }^{\circ}\text{C}$ SPU2.5 samples have the highest storage modulus while SPU1.5 has the lowest value. On the other hand, when temperature rises to $25\text{ }^{\circ}\text{C}$ and $37\text{ }^{\circ}\text{C}$, storage modulus values have the following order: SPU1.5 > SPU2.5 > SPU5 (Table 3). Since the SS crystallinity has an impact on the value of the storage modulus, higher SS crystallinity yields a higher magnitude of E' at rubbery plateau.²⁹ Both E' and E'' obtained at $25\text{ }^{\circ}\text{C}$ and $37\text{ }^{\circ}\text{C}$ showed a decrease with increase in HDI content demonstrating an increase in phase mixing and decreasing SS crystallinity. When E'' values are

analyzed, α_a peak corresponding to the SS phase and α_m peak corresponding to the T_g of the mixture phase are very obviously noticeable for all SPU samples.

2.5. Results of XRD analysis

Crystalline structures of all SPUs obtained in the range of $2\theta = 5^\circ$ – 40° by XRD analysis are given in Figure 6. Characteristic peaks of PCL-diol (semi-crystalline) are reported at $2\theta = 21.5^\circ$, 22° , 23.5° in the literature.³⁰ For all synthesized PU samples, broad peak between $2\theta \sim 20.28^\circ$ – 20.88° was observed in the XRD spectrum due to the soft crystalline phase. Crosslinking of polymers limits the flexibility and movement of chains; however, SS parts long enough to crystallize were still present in the structures of SPU samples. In XRD spectra, it was observed that all PU samples had PCL-diol crystal peaks at the same place ($2\theta = 20.4^\circ$). However, the intensity of the peaks changed as in the given order: SPU1.5 > SPU2.5 > SPU5 due to the different amount of SS crystallinity. The sample which has the highest crystallinity was SPU1.5. In the literature, in the XRD spectra of SPUs, the peaks at around $2\theta = 11^\circ$ and $2\theta = 19^\circ$ belong to the crystallinity of different crystallographic planes.³¹ No sharp peak for HS crystallinity was observed for SPU1.5 and SPU2.5 samples, but a small peak at around $2\theta = 11^\circ$ was detected because of the different crystalline parts assigned as HS in polymer structure.

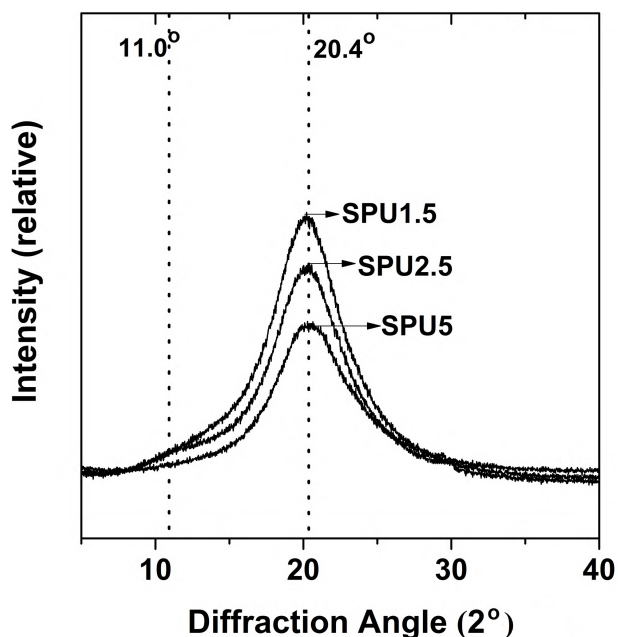


Figure 6. The XRD curves of different SPU films in the range between 5° and 40° .

2.6. Mechanical properties

Table 4 summarizes the mechanical properties of the synthesized SPUs. It is seen that alteration in hydrogen bonding, amount of crystallinity, and crosslinking degree due to variation in HDI content, tensile properties differ among SPUs. Values of ultimate tensile strength, elastic modulus, and elongation at break range from 1.9 MPa to 14.3 MPa, from 2.9 MPa to 9.9 MPa, and from 85.9% to 1170.0%, respectively. The results obtained for SPUs are in agreement with the literature in which it was given that tensile strength and modulus values increased from 21 MPa to 27 MPa and from 1.9 MPa to 3.2 MPa, respectively; and elongation at break decreased from 1200% to 545%.²⁸

Table 4. Tensile properties of SPU films (\pm SD, n = 5).

Sample	UTS (MPa)	E (MPa)	EAB (%)	HS content (wt%)
SPU1.5	14.3 \pm 4.1	2.9 \pm 0.5	1171.0 \pm 114.9	17
SPU2.5	1.9 \pm 0.3	4.5 \pm 0.4	106.1 \pm 34.9	25
SPU5	2.7 \pm 0.4	9.9 \pm 1.5	85.9 \pm 21.4	40

The increase in elastic modulus with increasing HS content from 17 to 40 wt.% can be explained by the increase in crosslinking density. For the SPU1.5 sample three different regimes are clearly noticeable. First, pure elastic deformation of normal elastomers; secondly, plastic deformation at strains between 200% to 600%; and thirdly, an upswing caused by induced crystallization of SS at strains above 600% were observed.³² For SPU5, although it revealed the lowest phase separation (also supported with IR spectrum), Young's modulus (E) increased while ultimate tensile strength (UTS) and percent elongation decreased with increasing crosslinks between polymer chains due to its higher HDI content. Interestingly, ultimate tensile strength and elongation showed a decreasing tendency while elastic modulus increased. In this case, the increase in crosslinking degree resulted in an increase in elastic deformation. Accordingly, the resulting mechanical properties of SPUs are not only attributed to separated or mixed phase morphology but also to the amount of crosslinking.

The characteristics of the crosslinked polymers are governed by their relative concentration and the length between the crosslinking points. For a crosslinked polymer, if the attractions between the polymer chains are strong then the chain length between the crosslink points gets shorter. This means that as the HS content increases, as a result, high modulus will be observed for this type of samples. The higher UTS and E values of SPU5 compared to those of SPU2.5 can be explained in this way. On the other hand, SPU1.5 demonstrated the highest values of UTS which can be explained by the larger free volume fractions and strong cohesiveness of HSs. This might be raised due to better phase separation and protection of crystalline parts of SSs. PCL-diol crystallinity strongly affected the mechanical properties. When comparing polymer samples, it is clear that undeformed crystalline structures of SS in polymer structure strongly enhanced the UTS value of SPU1.5 sample. Moreover, crosslinking increased elastic modulus. Thus, by varying the chemical structure of a polymer, it is possible to obtain various polymers possessing different mechanical properties, as this is reported in the literature for phase-separated SPUs.^{33–35}

In conclusion, solvent- and catalyst-free SPUs were successfully synthesized by the direct reaction of PCL-diol with different amounts of HDI. Crosslinking between polymer chains was achieved via formation of allophanate and/or biuret linkages due to the presence of excess HDI. Resulted polymers were characterized by FTIR-ATR, AFM, DSC, DMA, XRD, and mechanical tester and the obtained results were evaluated and discussed by taking the initial composition as the base. Meanwhile, it was attempted to explain the composition-property relationship. Alteration in the NCO to OH ratio caused substantial effect on phase segregation which also caused variations in overall properties of the material. Deconvolution of FTIR spectra showed that an increase in the HDI content resulted in distribution of HS in SS. Increase in HDI content increases the crosslinking and causes a change in N–H groups present in HS by increasing the amount of free N–H groups. This leads to better mixing of HS and SS and therefore causes disruption of SS crystallinity that is also confirmed by the AFM images and DSC results. Higher content of HS causes a decrease in the number of segmental relaxations as observed in DMA results. Higher crosslink density shortens the chain length between the crosslink points and therefore makes the material stiffer with lower elongation values. It can be concluded that increase in HS

content in this type of PUs can alter the properties significantly arising from mixing of HS with SS domains. Therefore, it would be possible to prepare environmentally friendly SPU products with the desired properties without using toxic ingredients.

3. Experimental

3.1. Materials

In the synthesis of PU, HDI and PCL-diol (M_n : 1250 g mol⁻¹), produced by Sigma-Aldrich (St. Louis, Missouri, USA), were used. HDI was kept at 4 °C and handled carefully since it has very reactive isocyanate groups.

3.2. Synthesis of segmented polyurethanes and film preparation

Three types of SPUs were synthesized by one-shot polymerization changing the initial molar ratio of HDI to PCL-diol as described previously.³⁶ Shortly, PCL-diol was vacuumed for 2 h at 80 °C in order to remove moisture and then nitrogen was purged for 1 h at 90 °C. HDI was added dropwise and the reaction was carried out for 6 h under nitrogen atmosphere at 90 °C. The viscous prepolymer was transferred into glass petri dishes and cured at 95 °C in a vacuum oven. The progress of the polymerization reaction was followed by getting FTIR analysis of the samples which were smeared on a KBr pellets. When the free isocyanate peak disappeared (~7 days), the glass petri dishes were put into boiling water for extended curing process for 5 min. The SPU films (thickness 200–300 µm) were then removed from the molds and dried in vacuum oven. Schematic representation of diisocyanate terminated PU synthesis and formation of crosslinks via allophanate and biuret linkages during curing are shown in Figure 7. Theoretical values of HS content (as wt.%) were calculated by using Eq. (1) given below:

$$HS(wt.\%) = [(n_{HDI} \times M_{HDI}) / (n_{HDI} \times M_{HDI} + n_{PCL-diol} \times M_{PCL-diol})] \times 100, \quad (1)$$

where average molecular weight of the reagents (g mol⁻¹) are designated as M and mole numbers used in the experiment are termed as n. Three types of SPUs were synthesized and named as: SPU1.5 (with 17% HS), SPU2.5 (with 25% HS), and SPU5 (with 40% HS), where the numbers after SPU demonstrate molar ratio of diisocyanate to polyol (for example, the mol ratio of HDI/PCL-diol = 1.5 for SPU1.5 sample).

3.3. Characterization methods

Chemical compositions and the progress of polymerizations were examined by FTIR (Perkin Elmer Spectrum 65 BX-FTIR-ATR, Massachusetts, USA). IR spectra of SPU films were obtained with ATR attachment having ZnSe crystal in the frequency range of 4000–600 cm⁻¹ by recording 64 scans where the resolution was 4 cm⁻¹. Phase and height images of the samples were obtained by AFM (Nanoscope Vecoo MultiMode V Santa Barbara, USA) performing tapping mode using a Silicon tip. AFM results were examined with free Gwyddion data analysis software.³⁷

For thermal analysis, DSC (Scinco DSC N-650, Seoul, Korea) was used. Approximately 15–20 mg of polymer sample was sealed in aluminum capsule and heated under nitrogen atmosphere with a scanning rate of 10 °C min⁻¹ over the temperature range from –100 °C to 200 °C.

DMA was performed with DMA instrument (Perkin Elmer Pyris Diamond, Shelton, USA) in order to examine the thermo-mechanical properties. The measurements were carried out in an oscillatory tension mode

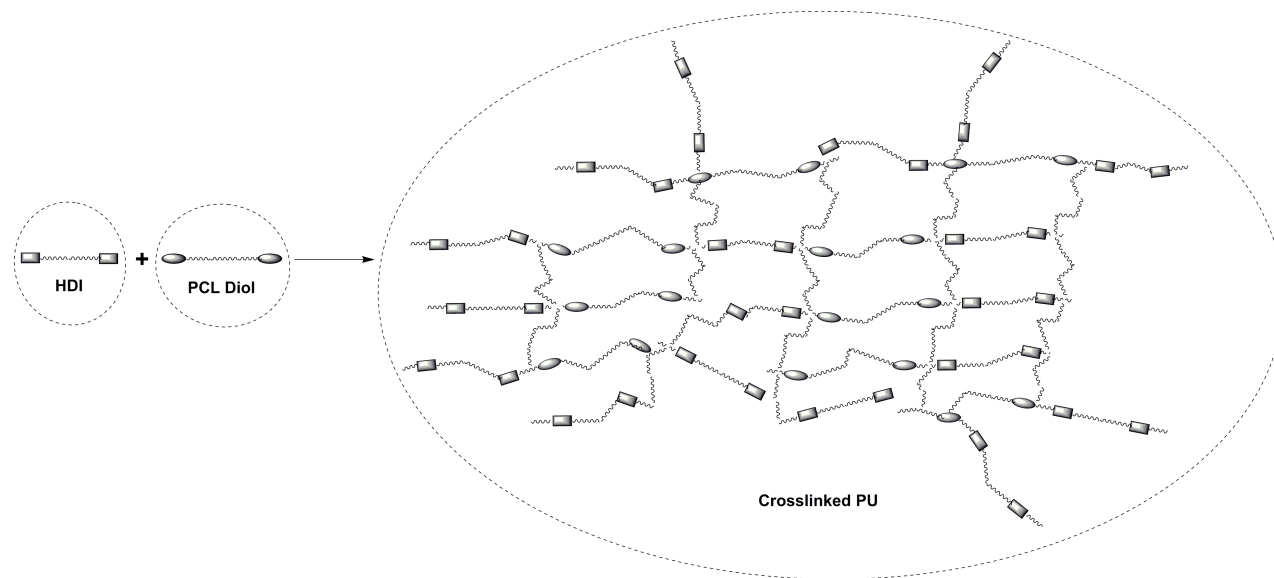


Figure 7. Schematic representation of synthesis of NCO-terminated and crosslinked SPU films.

where the oscillation frequency was 1 Hz, the heating rate was $5\text{ }^{\circ}\text{C min}^{-1}$, and the system was under nitrogen atmosphere. Dynamic mechanical data of the specimens were analyzed in the temperature range of $-100\text{ }^{\circ}\text{C}$ to $150\text{ }^{\circ}\text{C}$.

XRD measurements were conducted by using a X-ray diffractometer (Rigaku Ultima-IV, Tokyo, Japan) equipped with a copper target ($\lambda = 1.54\text{ \AA}$, 40 kV, 30 mA) and a graphite monochromator. The samples were placed on a holder and scanned in the range of $2\theta = 5^{\circ}\text{--}80^{\circ}$ at a speed of $2^{\circ}\text{ min}^{-1}$.

Tensile properties of SPU films ($10\text{ mm} \times 50\text{ mm} \times 0.2\text{ mm}$) were examined by a mechanical testing instrument (Lloyd Instruments, Ltd., Fareham, UK) having a crosshead speed of 10 mm min^{-1} . UTS, E, and percent elongation at break (EAB%) values were calculated from the stress versus strain graphs obtained from the instrument.

Acknowledgments

The authors are grateful to Engin Özkol (Department of Chemical Engineering, METU, Turkey) for his help in the use of Peakfit Version 4.12 software and thank the METU Central Laboratory for characterization analyses of DMA and XRD. This study was supported by METU-BAP Research Grants.

References

1. Yilgor, I.; Yilgor, E.; Wilkes, L. G. *Polym.* **2015**, *58*, A1-A36.
2. Burke, A.; Hasirci, N. *Adv. Exp. Med. Biol.* **2004**, *553*, 83-101.
3. Sheth, J. P.; Klinedinst, D. B.; Wilkes, G. L.; Yilgor, I.; Yilgor, E. *Polym.* **2005**, *46*, 7317-7322.
4. Drobny, J. G. In *Handbook of Thermoplastic Elastomers*; Elsevier: Oxford, UK, 2014, pp. 215-234.
5. Sudemen, M. B.; Onen H. A. *Turk. J. Chem.* **2017**, *41*, 630-647.
6. Ajili, S. H.; Ebrahimi, N. G.; Soleimani, M. *Acta Biomater.* **2009**, *5*, 1519-1530.

7. Hung, K. C.; Tseng, C. S.; Dai, L. G.; Hsu, S. *Biomaterials*. **2016**, *83*, 156-168.
8. Valerio, A.; Conti, D. S.; Araujo, P. H.; Sayer, C.; Rocha, S. R. *Colloids Surf. B Biointerfaces* **2015**, *135*, 35-41.
9. Gogolewski, S.; Gorna, K. *J. Biomed. Mater. Res. A*. **2007**, *80*, 94-101.
10. Pereira, I. H. L.; Ayres, E.; Patricio, P. S.; Goes, A. M.; Gomide, V. S.; Junior, E. P.; Orefice, R. L. *Acta Biomater.* **2010**, *6*, 3056-3066.
11. Kara, F.; Aksoy, E. A.; Calamak, S.; Hasirci, N.; Aksoy, S. *J. Bioact. Compat. Polym.* **2016**, *31*, 72-90.
12. Trinca, R. B.; Abraham, G. A.; Felisberti, M. I. *Mater. Sci. Eng. C*. **2015**, *56*, 511-517.
13. Marcos-Fernandez, A.; Abraham, G. A.; Valentin, J. L.; San Roman, J. *Polym.* **2006**, *47*, 785-798.
14. Kiziltay, A.; Marcos-Fernandez, A.; San Roman, J.; Sousa, R. A.; Reis, R. L.; Hasirci, V.; Hasirci, N. *J. Tissue Eng. Regen. Med.* **2015**, *9*, 930-942.
15. Park, H. S.; Gong, M. S.; Park, J. H.; Moon, S.; Wall, I. B.; Kim, H. W.; Lee, J. H.; Knowles, J. C. *Acta Biomater.* **2013**, *9*, 8962-8971.
16. Modarresi-Alam, A. R.; Rostamizahed, M.; NAJAFI P. *Turk. J. Chem.* **2006**, *30*, 269-276
17. Hasirci, N.; Aksoy, E. A. *High Perform. Polym.* **2007**, *19*, 621-637.
18. Park, H. S.; Gong, M. S.; Knowles J. C. *J. Mater. Sci. Mater. Med.* **2013**, *24*, 281-294.
19. Heijkants, R. G. J. C.; van Calck, R. V.; van Tienen, T. G.; de Groot, J. H.; Buma, P.; Pennings, A. J.; Veth, R. P. H., Schouten, A. J. *Biomaterials*. **2005**, *26*, 4219-4228.
20. Bil, M.; Ryszkowska, J.; Woźniak, P.; Kurzydłowski, K. J.; Lewandowska-Szumieł, M. *Acta Biomater.* **2010**, *6*, 2501-2510.
21. Yilgor, I.; Yilgor, E.; Guler, I. G.; Ward, T. C.; Wilkes, G. L. *Polym.* **2006**, *47*, 4105-4114.
22. Queiroz, D. P.; de Pinho, M. N.; Dias, C. *Macromolecules*. **2003**, *36*, 4195-4200.
23. Romanova, V.; Begishev, V.; Karmanov, V.; Kondyurin, A.; Maitz, M. F. *J. Raman Spectrosc.* **2002**, *33*, 769-777.
24. Liu, J.; Ma, D. *J. Appl. Polym. Sci.* **2002**, *84*, 2206-2215.
25. Varnell, D. F.; Runt, J. P.; Coleman, M. M. *Macromolecules*. **1981**, *14*, 1350-1356.
26. Faria M., Pinho M. N. *European Polymer Journal*. **2016**, *82*, 260-276
27. Van Bogart, J. W. C.; Lilaonitkul, A.; Cooper, S. L. *J. Macromol. Sci. Phys. B*. **1980**, *17*, 267-301.
28. Wang W., Guo Y., Otaigbe J. U. *Polymer*. **2008**, *49*, 4393-4398
29. Reddy, T. T.; Hadano, M.; Takahara, A. *Macromol. Symp.* **2006**, *242*, 241-249.
30. Piacibello, W.; Sanavio, F.; Garetto, L.; Severino, A.; Bergandi, D.; Ferrario, J.; Fagioli, F.; Berger, M.; Aglietta, M. *Blood*. **1997**, *89*, 2644-2653.
31. Trovati, G.; Sanches, E. A.; Neto, S. C.; Mascarenhas, Y. P.; Chierice, G. O. *J. Appl. Polym. Sci.* **2010**, *115*, 263-268.
32. Grady B. R.; Cooper, S. L. In *Science and Technology of Rubber*; Eirich, F. R. Eds. Academic Press: New York, USA, 1978, pp. 555-617.
33. Silver, J. H.; Myers, C. W.; Lim, F.; Cooper, S. L. *Biomaterials*. **1994**, *15*, 695-704.
34. Li, C.; Speckhard, T. A.; Yu, X.; Cooper, S. L. *J. Polym. Sci. Polym. Phys. Ed.* **1988**, *26*, 315-337.
35. Yang, C. Z.; Li, C.; Ding, Y. S.; Cooper S. L. *J. Polym. Sci. Polym. Phys. Ed.* **1991**, *29*, 75-86.
36. Guney, A.; Hasirci, N. *J. Appl. Polym. Sci.* **2014**, *131*, 39758.
37. Nečas, D.; Klapetek, P. *Cent. Eur. J. Phys.* **2012**, *10*, 181-188.